Development and Preliminary Testing of a High Precision Long Stroke Slit Change Mechanism for the SPICE Instrument

Gabriel Paciotti*, Martin Humphries**, Fabrice Rottmeier* and Luc Blecha*

Abstract

In the frame of ESA's Solar Orbiter scientific mission, Almatech has been selected to design, develop and test the Slit Change Mechanism of the SPICE (SPectral Imaging of the Coronal Environment) instrument. In order to guaranty optical cleanliness level while fulfilling stringent positioning accuracies and repeatability requirements for slit positioning in the optical path of the instrument, a linear guiding system based on a double flexible blade arrangement has been selected. The four different slits to be used for the SPICE instrument resulted in a total stroke of 16.5 mm in this linear slit changer arrangement.

The combination of long stroke and high precision positioning requirements has been identified as the main design challenge to be validated through breadboard models testing. This paper presents the development of SPICE's Slit Change Mechanism (SCM) and the two-step validation tests successfully performed on breadboard models of its flexible blade support system.

Introduction

While classical space mechanism design for significant displacements are generally based on linear or rotational sliding contact guiding systems, the optical cleanliness requirements of the SPICE instrument has channelled the selection of a flexible guiding system for supporting the slit changer inside the optical cavity, and the use of an actuation mechanism hermetically separated from it. Rotational slit changers concepts have been investigated and rejected due to the need of sliding contact feedthroughs, the presence of unwanted total optical obscuration of the instrument during slit changes, the elevated angular resolution to meet the position accuracy, and/or general geometrical constraints.

The selected linear Slit Change Mechanism design is presented in Figure 1. The slit carrier is supported by a pair of parallel metallic blades held by an external frame. The linear actuator design, separated by a hermetic metallic bellows assembly from the optical chamber, consists of the combination of a stepper motor and a satellite roller screw reduction drive. The mechanical link between the suspended slit assembly and the actuator is provided by a compliant rod connection.

The required total stroke of the linear actuator is 16.5 mm for the positioning of four different slits in the instrument's line of sight, requiring a highly flexible blade system for precise guiding over the full displacement range of the slit carrier. The requirement on the maximum induced translational and rotational inaccuracies, as well as their repeatability over life, are summarized in Table 2. The most demanding requirement is the positioning of the slit on the beam axis of the instrument (in X and Y) and the rotation around the Y-axis with the corresponding repeatability.

Considering these highly demanding performances to be demonstrated over 54000 cycles, a two-step breadboard model validation test program has been initiated before full SCM mechanism validation at qualification level.

* Almatech, EPFL – Innovation Park, Lausanne, Switzerland

** SpaceMech Ltd., Westbury-on-Trym, Bristol, U.K.

Table 1. Contamination requirements for the SCM mechanism

Contamination Type	Unit	Inside optical cavity	Outside optical cavity
Particulate (PAC)	ppm	30	100
Molecular (MOC)	ng/cm^2	50	100

Table 2. Positioning accuracy and repeatability requirements over 16.5-mm Z-displacement

Direction	Positioning accuracy	Repeatability
X translation	±10 µm	±5 µm
Y translation	±50 µm	±3 µm
Z translation	±80 µm	±30 µm
Rotation around X	±5 arcmin	±30 arcsec
Rotation around Y	±50 arcsec	±25 arcsec
Rotation around Z	±10 arcmin	±5 arcmin

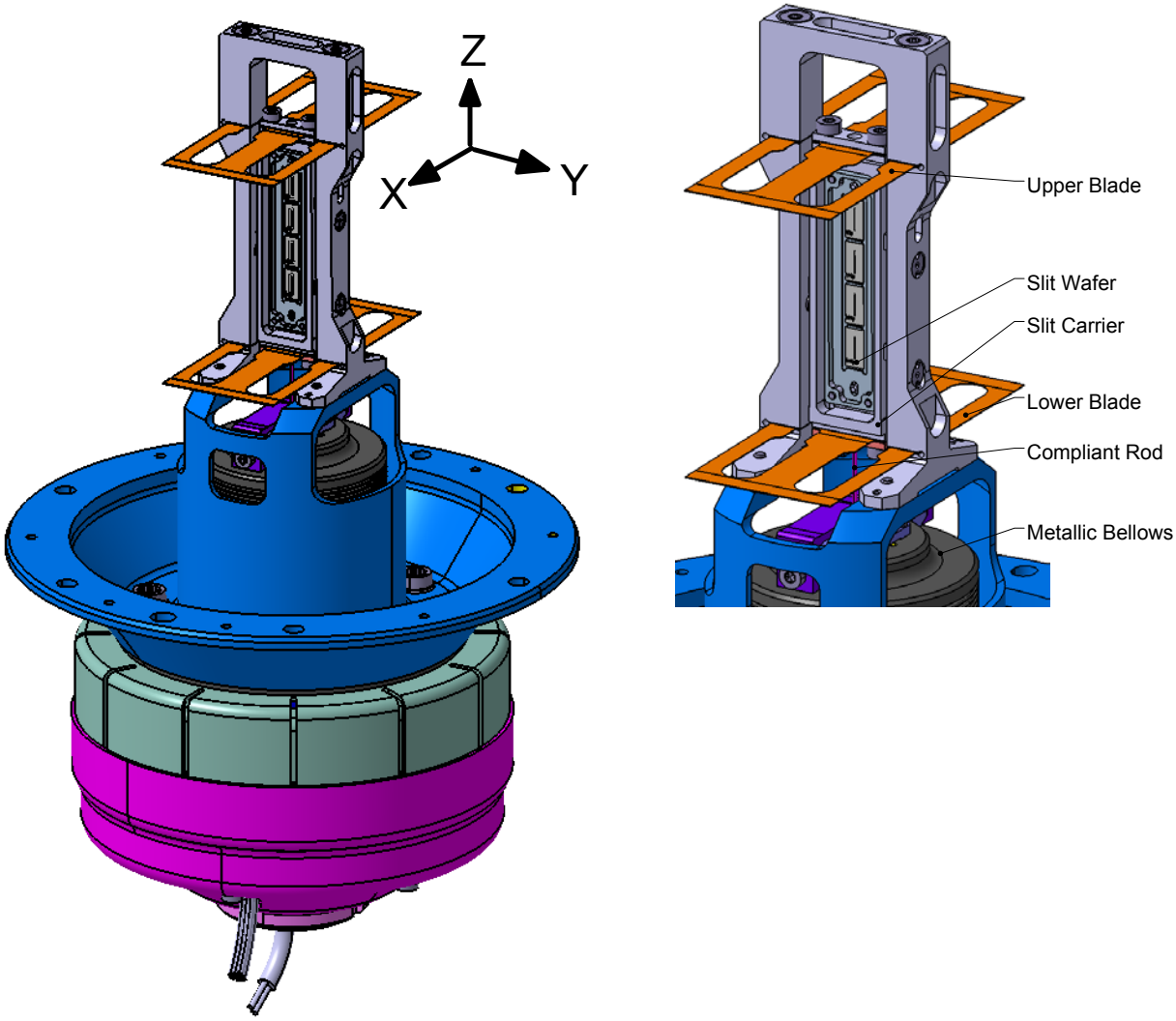

Figure 1. Linear Slit Change Mechanism design

Flexible Guiding System Design

The flexible guiding system of the slit carrier is provided by a parallel blade arrangement illustrated in Figure 1. With no relative motion between contacting parts, the blade arrangement is free of any friction or wear as well as need for lubrication. Consequently, it inherently prevents the generation of particles or contaminants, one of the main design drivers with respect to the optical cavity cleanliness requirement defined in Table 1. The flexible blades are dimensioned such to limit the deformation stresses and subsequently the creep impact, ensuring the repeatability of the positioning over the full stroke of the slit carrier and operational lifetime.

In order to minimize thermo-elastic deformation-induced positioning inaccuracies over the wide operational thermal environment range of -30°C to +60°C of the SCM, all parts structurally supporting the slits from the instrument interface are designed in the same material, which is a titanium alloy.

Each blade is cut out of a thin titanium sheet using a photo-etching process to ensure high precision dimensions, manufacturing tolerances, and reproducibility. This is a key element in the precise guiding of this parallel flexure arrangement since it requires the assembly of several mechanical elements. The manufacturing tolerances of the blade support frame, slit carrier, and provided blade pin-alignment features are additional contributors to the precision guiding functionality of this system. Symmetry, parallelism and alignment of the flexible blades being a major driver in the positioning precision over the relatively long stroke, the characterization of the flex-blade guiding performances over the full stroke has been considered as the first step for the evaluation of the performance of the full mechanism. Initial characterization tests on a representative breadboard model have therefore been integrated in the validation test program of the SCM and are presented in this article.

Considering the importance of launch loads on space structural designs, the main drawback of such a thin blade parallel arrangement is the lateral load carrying capability (X-Y plane). While the presented design was compatible with the initial random specifications, their evolution have led to the integration of slit carrier displacement limiters (snubbers) between the slit carrier and blade support frame. This additional contact-free guiding feature is only provided in the launch configuration (slit 2 active) in order to limit the range of the provided tight clearance of 30 microns (in X & Y) over the axial direction Z. Their dimensioning is such to limit contact stresses and avoid generation of wear particles.

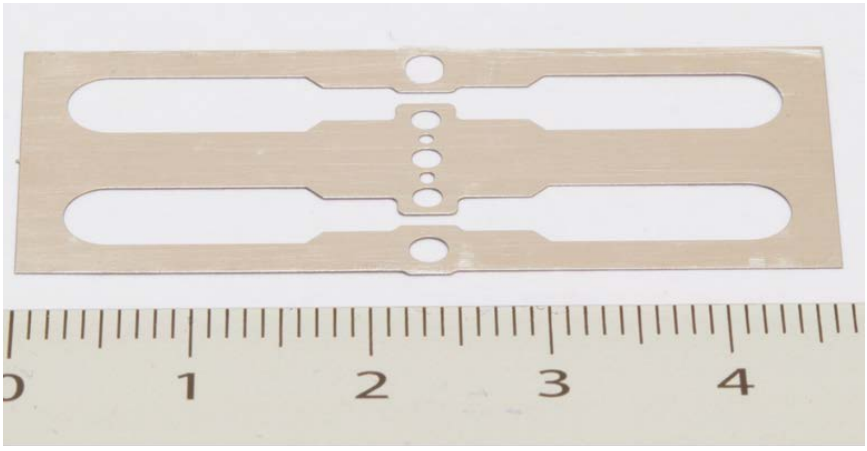

Figure 2. Titanium alloy flexible blade - scale in cm

Compliant Rod Connection Design

In order to meet the slit positioning accuracies for the complete SCM mechanism, the centering and alignment of the linear actuator axis with respect to the flexible guiding system axis is essential over the full design stroke. With the aim of limiting the transfer of alignment perturbations between the linear actuator and the flexible guiding system, a compliant rod connection has been integrated between these mechanical systems. The optimization of the compliant rod design is essential for the minimization of the alignment and repeatability requirements to be imposed on the more complex design of the linear actuator mechanism. For this reason, a sensitivity analysis of the flexible guiding system (including connection rod) to actuator misalignment has been performed using FEM analyses during the initial design phase. These analyses included the consideration of thermal distortion effects, linear and rotational misalignments, as well as residual torque input from the linear actuator and for each of the four nominal slit positioning conditions. The studied misalignment inputs and the combined output inaccuracies are presented in Table 3 and Table 4, respectively. Table 5 presents the minimum reduction factors between the considered perturbations and its outputs on the slit positioning.

Table 3. Linear actuator perturbation outputs

Direction	Source	Perturbation
X translation	misalignment	10 µm
Y translation	misalignment	10 µm
Rotation around X	misalignment	1 arcmin
Rotation around Y	misalignment	1 arcmin
Rotation around Z	misalignment	30 arcmin

Table 4. Total inaccuracies of slit positioning due to actuator input perturbations and thermal effects (absolute values)

Direction	Unit	required	Slit 1	Slit 2 active	Slit 3	Slit 4
X translation	µm	±10	2.04	2.77	3.5	4.22
Y translation	µm	±50	1.19	1.6	2.01	2.42
Z translation	µm	±80	30.2	27.9	25.5	23.1
Rotation around X	arcmin	±5	0.26	0.26	0.26	0.26
Rotation around Y	arcsec	±50	27	27	27	27
Rotation around Z	arcmin	±10	0.05	0.06	0.07	0.08

Table 5. Minimum reduction factor on slit positioning accuracy due to actuator perturbations

Direction	Reduction factor
X translation	2.37
Y translation	4.13
Rotation around X	3.87
Rotation around Y	2.2
Rotation around Z	392

Note that the maximum displacement values presented in Table 4 are based on a single geometrical configuration consisting of the alignment of slit 2 on the optical axis (active slit), such that the results include the Z-offset of the other slits. Therefore, the lowest slit (slit 4) being the furthest away from the active slit, it presents the maximum absolute inaccuracies values in a worst case approach.

Based on the defined perturbation inputs from the linear actuator, the slit positioning combined responses are all compliant to the required values. More detailed analyses of the FEM model deformation results have shown that the major contribution to the X translation is a slight tilting of the whole blade support frame that has been stiffened in the QM/FM design. The transmission of X and Y misalignment are reduced by a minimum factor of 2.37 from the actuator to the slit positioning as shown in Table 5.

Z displacement inaccuracies are governed by the thermo-elastic behavior along this axis over the wide operational temperature range and the structural path from the SCM mechanical interface to the active slit position for this axis-symmetric mechanism design. All the parts involved in this structural chain are designed in the same material, titanium, such that the Z displacement inaccuracies are easily temperature compensated by the linear actuator control system. Mainly for this purpose, the resolution of the stepper motor driven linear actuator has been set to 5 microns; see the following paragraph for more detailed information on the linear actuator design. The design limitation for the compliant rod is its buckling stability during the dimensioning vibration loads, which provides the limit for the decoupling features of this compliant element.

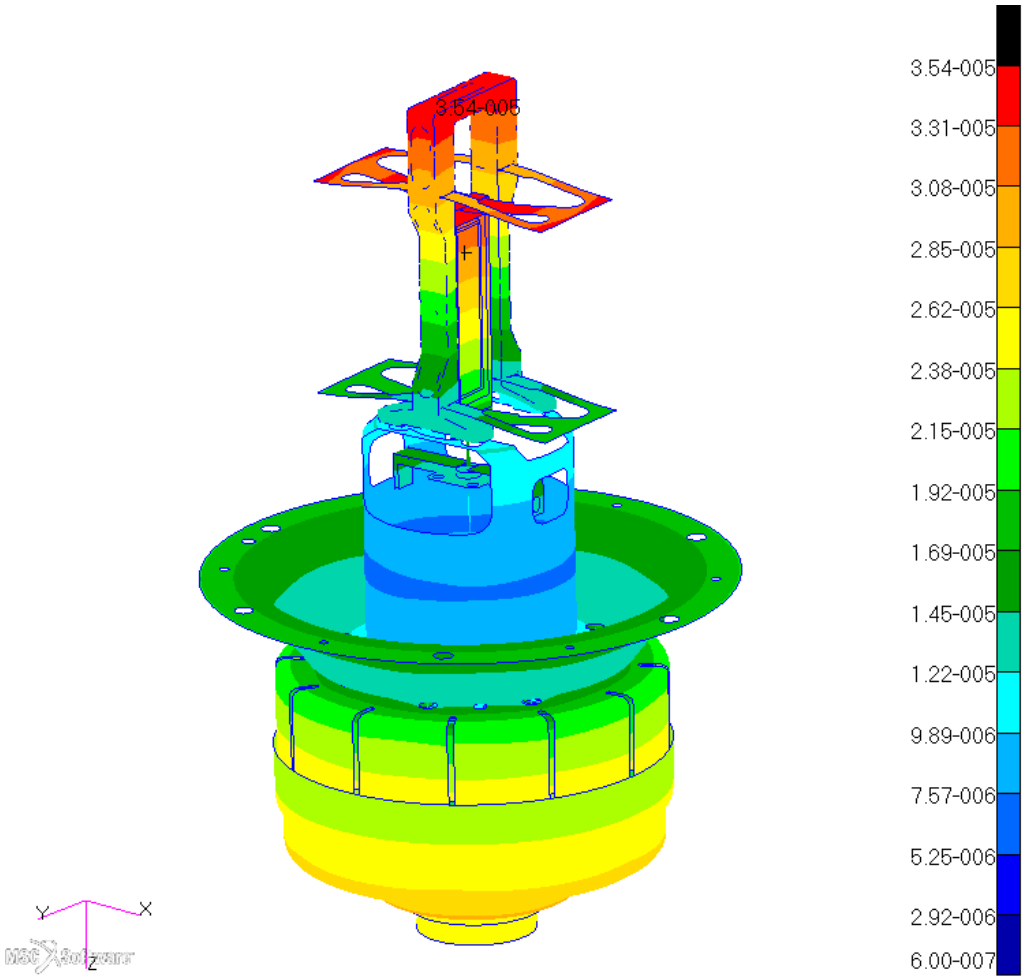

Figure 3. SCM temperature induced displacements from FEM sensitivity analyses over 50K – [m]

Linear Actuator Design

In order to drive the linear positioning of the suspended slit carrier, a space-qualified low-power and reduced-thickness stepper motor has been selected and combined with a custom-designed satellite roller screw. The soft-preloaded satellite roller screw has been designed by Rollvis SA in close collaboration with Almatech to allow a direct and compact integration of the motor and bearings on the roller screw shaft, targeting the compliance to the required positioning accuracies and repeatability over the design life of the mechanism.

The advantages of a satellite roller screws over ball screw are mainly a higher number of points of contact that distributes the transmitted loads. This allows a higher static and dynamic load capacity, in particular during the launch environment. Moreover, it implies lower wear and longer lifespan which is one of the SCM's main design challenges and selection criteria. Another main advantage of satellite roller screw over ball screw linear drives are that they allow a more compact design. Furthermore, the ability to select at will the pitch of the planetary roller screw independently to available ball sizes has contributed to the advantages of such a solution. Based on the 200 steps per revolutions design of the selected motor, this feature allowed to set the resolution of the linear actuator to 5 microns per motor step, or 1 mm per rotor revolution. Finally, the design of the satellite roller screw dedicated to the SCM allowed the integration of custom mechanical end-stops directly on the non-rotating lead screw.

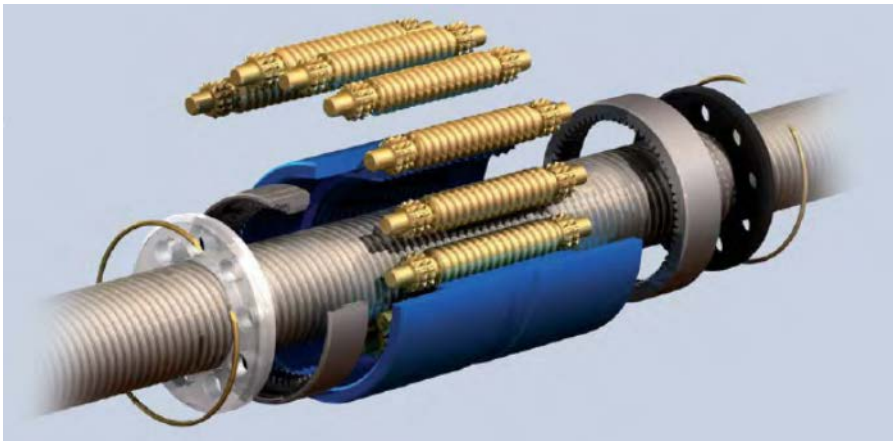

Figure 4. Satellite screw design illustration (Courtesy of Rollvis SA)

With the aim of assessing the guiding accuracy of the lead screw, measurements were performed on commercial off-the-shelf satellite roller screws directly by the manufacturer of this component. These tests have shown that the oscillation of the lead screw around the nut axis is better than ±5 microns, confirming the selection of a satellite roller screw driving mechanism for a high precision positioning application such as the SCM. The off-axis error will be further reduced on custom-made systems especially designed for high-precision applications and by the matching of manufactured components resulting in the best final performances results.

The SCM's rotating assembly is supported by a pair of angular contact preloaded ball bearings in face-to-face configuration to lower the angular stiffness of the assembly and allow the integration of the bearing preloading systems on the outer rings.

In order to evaluate the guiding accuracy of the output lead screw of the fully assembled linear actuator and optimize the linear actuator design, a tolerance analysis has been performed. This study included the consideration of the all duplex bearing assembly parameters (type, size, tolerance class, arrangement, groove wobble, bearing seat coaxiality…) and all geometrical uncertainties due to the manufacturing of structural parts supporting the rotating equipment. Sensitivity analyses of these main parameters allowed

an optimization of the design and the definition of manufacturing tolerances for the most critical dimensions.

Figure 5 presents the tolerance analysis results for the baseline design configuration of the linear actuator and includes the roller screw's radial run-out values based on the maximum measured values on commercial off-the-shelf roller screws. The prediction of the total run-out of the linear actuator lead at its maximum extension is 16.1 microns which can only comply with the X-axis positioning accuracy requirement by considering the lateral decoupling effect of the connection rod (i.e. minimum factor of 2.37 in Table 5). The predicted angular runout results of the lead screw is compliant with the requirements, in particular considering the reduction of the angular deflection due to the connection rod's bending (minimum factor of 2.2).

In addition to the potential reduction of roller screw radial run-out on the custom SCM version, the static misalignment effect can be reduced by a precise alignment of the flexible guiding system's axis to the linear actuator control axis. This alignment feature has been integrated in the SCM FM design and corresponding mounting procedures to further enhance the final positioning accuracies. It consists of the alignment, using an optical measuring technique, and high precision shimming of the blade support frame, followed by the clamping of the compliant rod connection. This later being specially designed to avoid the transmission of coupling stress during assembly.

Considering the criticality of the compliant rod connection design on the performances of the SCM's positioning performances, it has been decided to assess its impact on the flexible guiding system using breadboard validation tests.

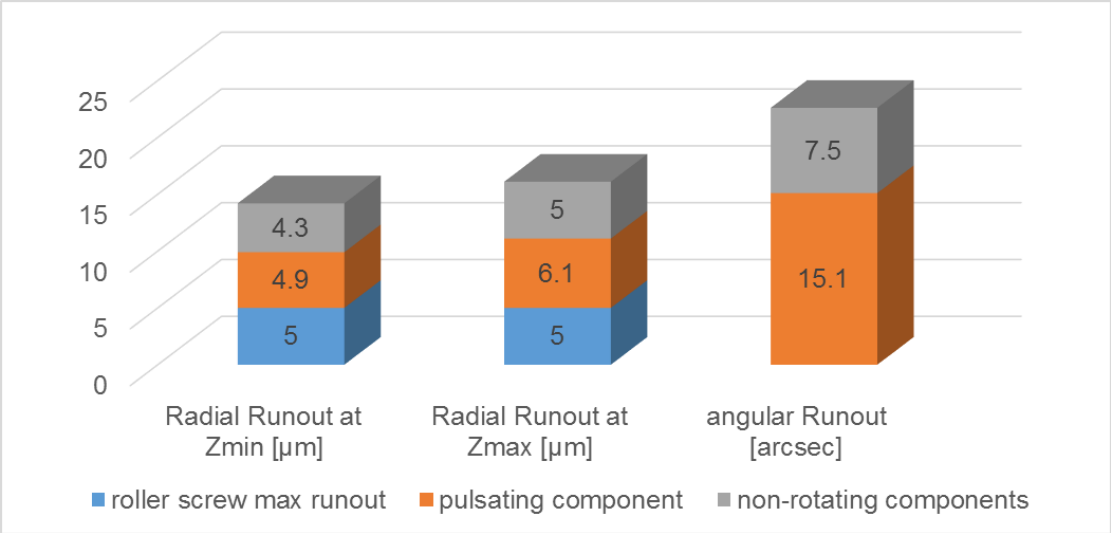

Figure 5. Final configuration tolerance analysis results

The positioning control of the SCM (along Z) is performed by step counts of the stepper motor. With the intention of allowing the initialization of the displacement control system, a high-precision switch (±1 µm) has been integrated in the SCM. It is triggered by the lower extremity of the lead screw as illustrated in Figure 6 and Figure 7.

Another key design challenge of the linear Slit Change Mechanism being its repeatability over the significant lifetime, careful attention has been given to the lubrication of the bearings and satellite roller screws. With the support of ESTL for the lubrication analyses (and for performing the lubrication of these components), lead lubricated bearings and hybrid lead/grease lubrication have been selected for the satellite roller screw.

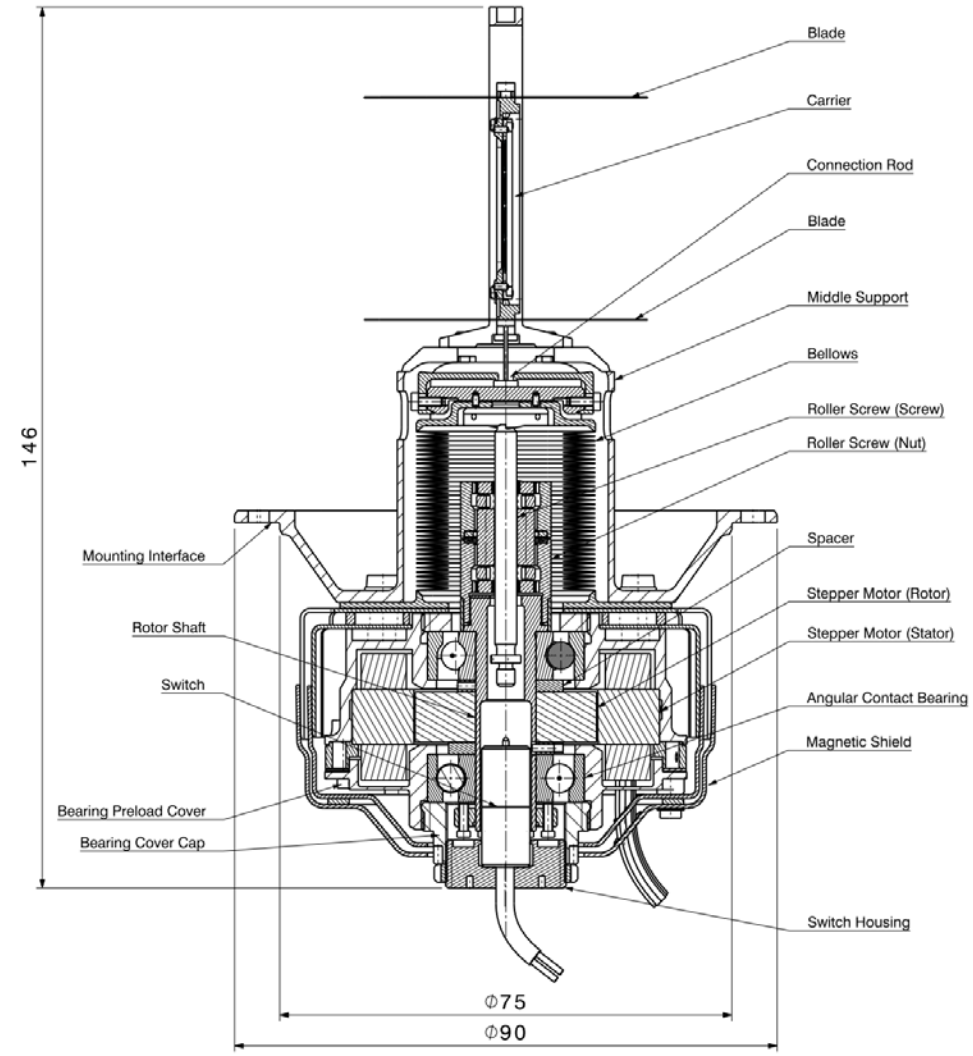

Figure 6. Cut view of the linear Slit Change Mechanism design – dimensions in mm

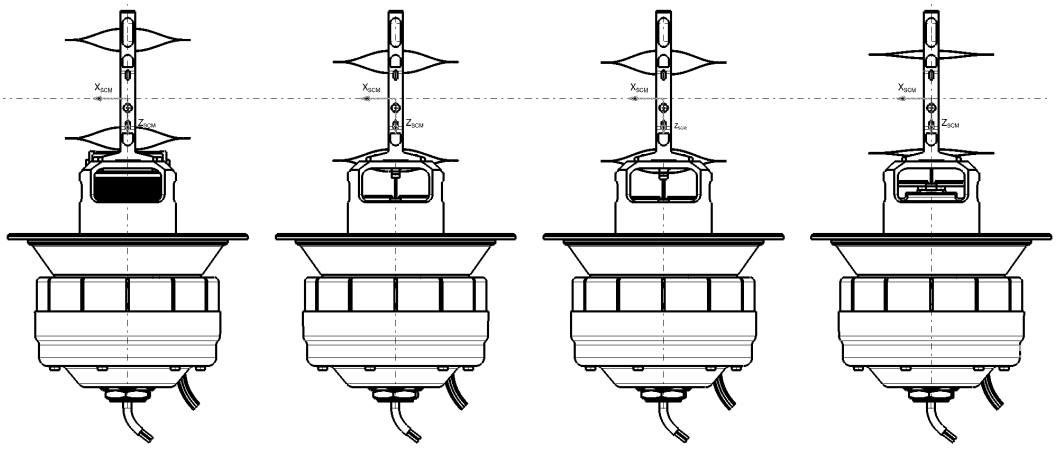

Figure 7. Linear Slit Change Mechanism design – configuration examples

Validation Test Program

In order to assess the positioning performances of the Slit Change Mechanism in a step by step approach, it has been decided to proceed with the following validation test strategy:

1. Characterization of the flexible guiding system performances over the full stroke
2. Assessment of the influence of the compliant rod connection on flexible guiding performances
3. Performance measurements of the full mechanism on the SCM QM

In this article, the test apparatus and results for the two derisking steps are presented and discussed. The initial breadboard model test results performed on the flexible guiding system are presented hereafter. They are followed by the characterization test results of the influence of the compliance rod connection on the slit positioning accuracy. The performance measurements for the full SCM mechanism are not presented in this article.

Flexible Guiding System Characterization Test Results

The initial breadboard tests were performed on a full-scale model of the flexible guiding mechanism, shown in Figure 8. These tests specifically aimed at measuring the geometrical positioning accuracy and repeatability over the full stroke for a limited number of cycles. The Z displacement was imposed using a steel wire tensioning system. Displacements were measured using two different high precision Laser Displacement Meters and rotations using a high-resolution Laser Diode Sensor Vector Autocollimator.

All X translation measurements were performed in a vertical configuration such to alienate gravity effects. The use of a traction system implied the need to perform +Z and –Z measurement tests separately and combine the test results.

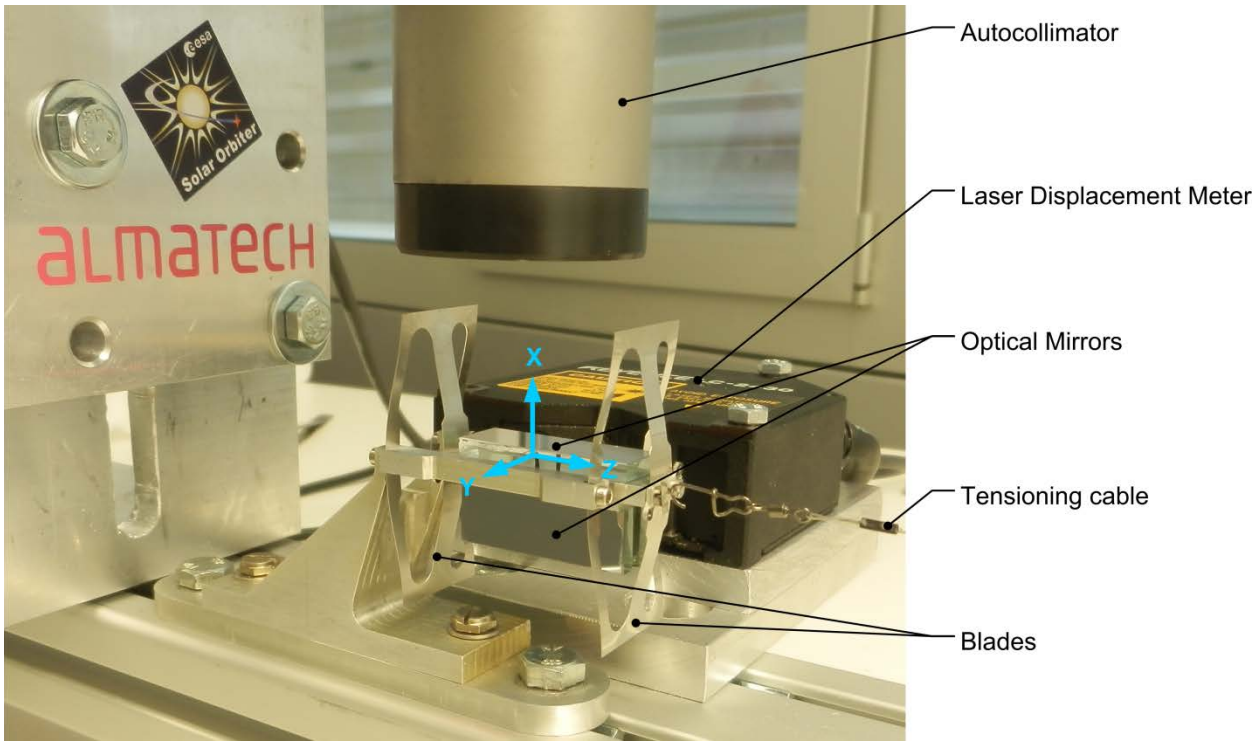

Figure 8. Breadboard model 1 test setup

Figures 9 and 10 present the slit carrier's displacement and rotational test results in function of the translation axis Z. High repeatability is observable between measured curves in each translation and rotation. All results are within the allowable limits with an exception for the $R_y(Z)$ tests results. Following these tests, it has been observed that the tensioning cable fixation lug was slightly bent, introducing a perturbation moment around the Y axis for the –Z direction. For the +Z direction, the deviation from the requirement have been attributed to the breadboard's blade alignment system that has been further enhanced for the following breadboard tests and QM/FM design.

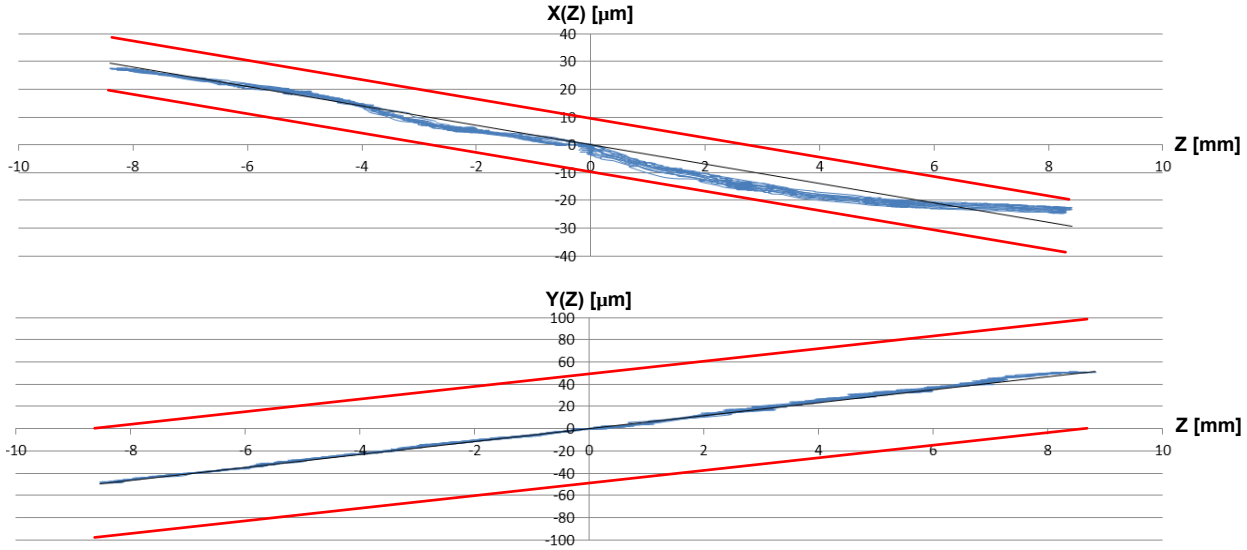

Figure 9. Slit carrier position in function of the Z in mm (biased by optical setup configuration)

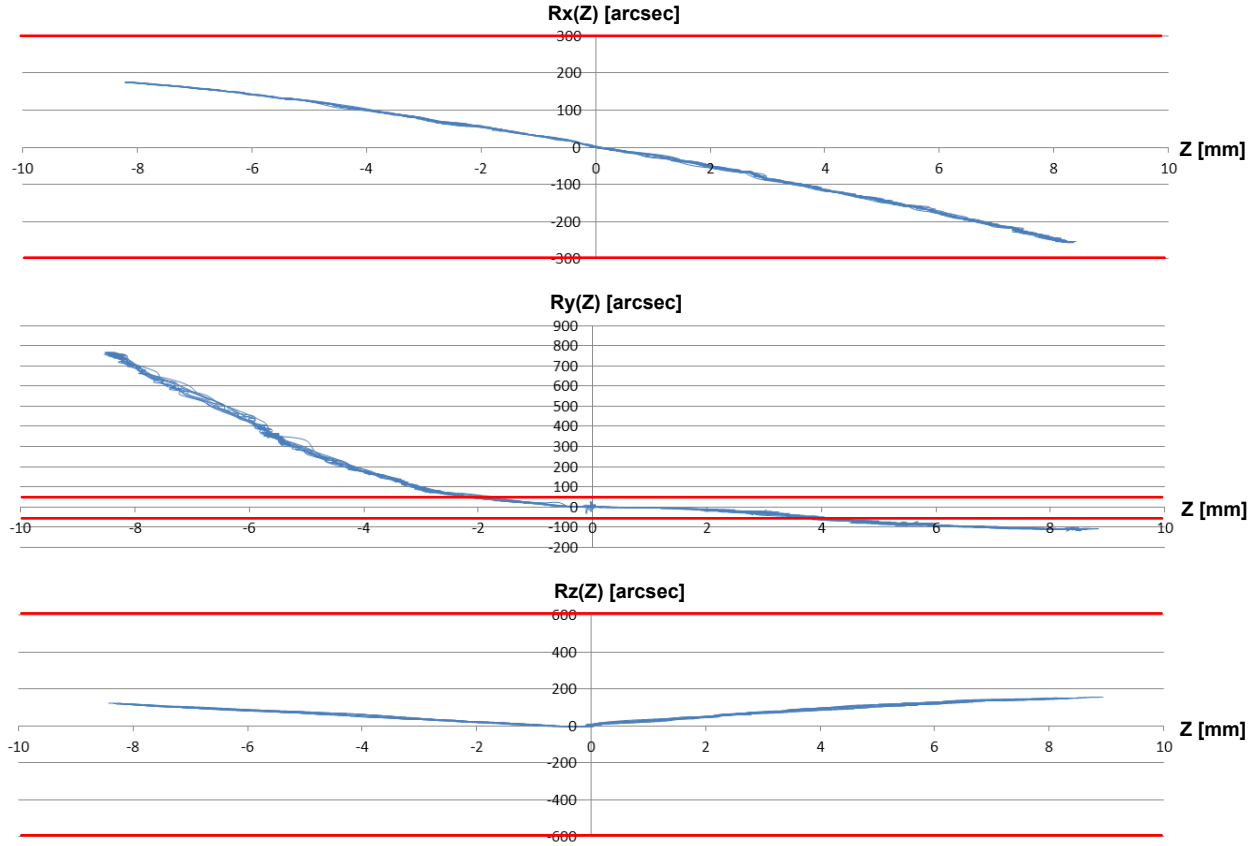

Figure 10. Slit carrier rotation in function of the Z-translation in mm

Table 6 summarizes the initial breadboard model test results performed on the flexible guiding system presented above.

Table 6. Max. positioning inaccuracy & worst case repeatability results from Z-displacement

Direction	Position accuracy		Repeatability	
	Measured	Required	Measured	Required
X translation	±7.2 µm	±10 µm	±2.17 µm	±5 µm
Y translation	±5.1 µm	±50 µm	±0.71 µm	±3 µm
Rotation around X	±4.28 arcmin	±5 arcmin	±3.65 arcsec	±30 arcsec
Rotation around Y	±768 arcsec	±50 arcsec	±5.14 arcsec	±25 arcsec
Rotation around Z	±2.60 arcmin	±10 arcmin	±0.11 arcsec	±5 arcmin

Flexible Guiding System Performance Test Results with Compliant Connection

The second set of breadboard tests were performed on a full-scale model of the flexible guiding mechanism including the compliant connection rod and its clamping system. All design improvements identified during the initial flexible guiding system tests, presented above, have been implemented in the flexible guiding system design of the second Breadboard Model. This second set of tests specifically aimed at measuring the geometrical positioning accuracy and repeatability over the full stroke for a limited number of cycles (10). The Z-displacement was imposed using a micrometer in a vertical configuration. Displacements in X, Y and Z were measured using three high-precision Laser Displacement Meters. Rotations were measured using two high-resolution Laser Diode Sensor Vector Autocollimators. The test apparatus for these measurements, shown in Figure 11, included the use of an optical table with pneumatic vibration isolation system.

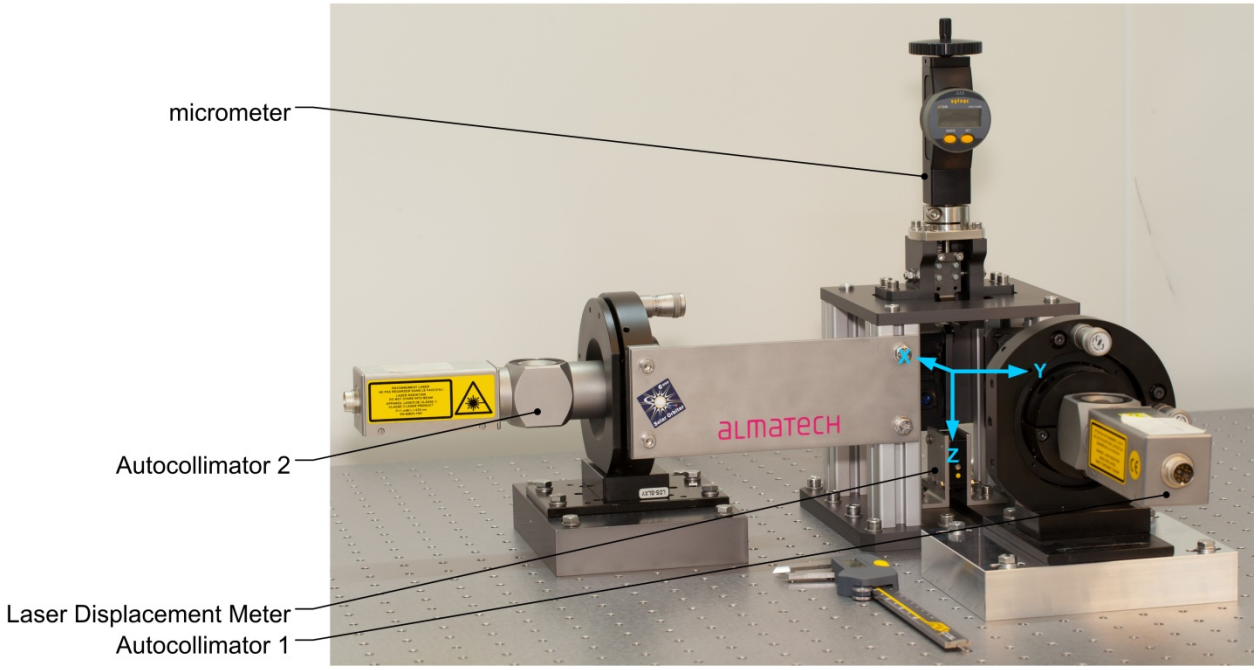

Figure 11. Breadboard model 2 test setup

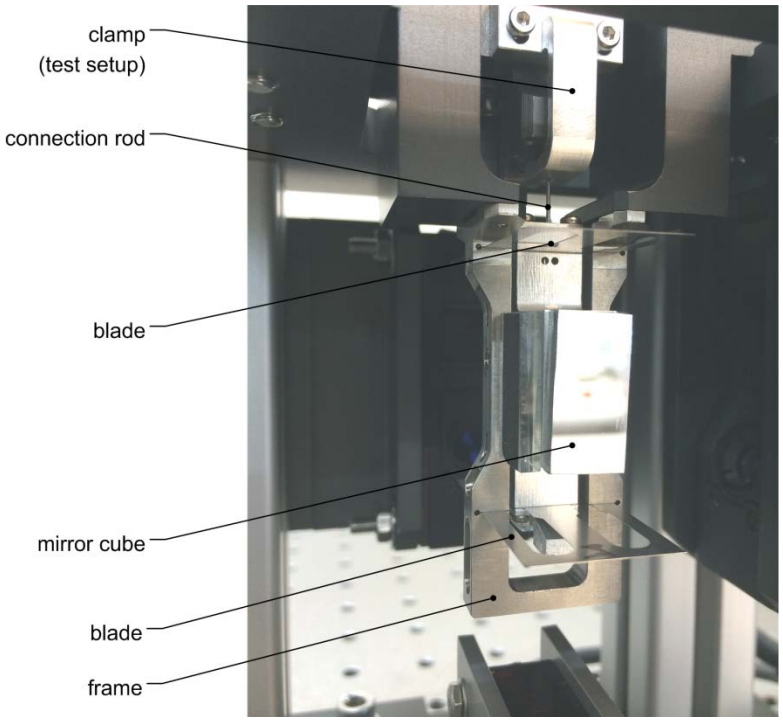

Figure 12. Breadboard model 2 flexible guiding system

Figures 13 and 14 present the slit carrier's displacement and rotational test results in function of the translation axis Z for the second test series (10 full strokes). Very high repeatability is observable between measured curves in each translation and rotation with a significant enhancement from the previous test result presented in Figures 9 and 10. The second set of results is well within the allowable limits with an exception for the $R_y(Z)$ test results. In the corresponding figure, the four slit positioning locations are represented as circles. At these discrete locations where the positioning and repeatability requirements are applicable, they are just met. The origin of the behavior of the rotation around Y over the full stroke can be attributed to either a misalignment of the flexible blades in the X direction or some dissymmetrical behavior of the flexible blades.

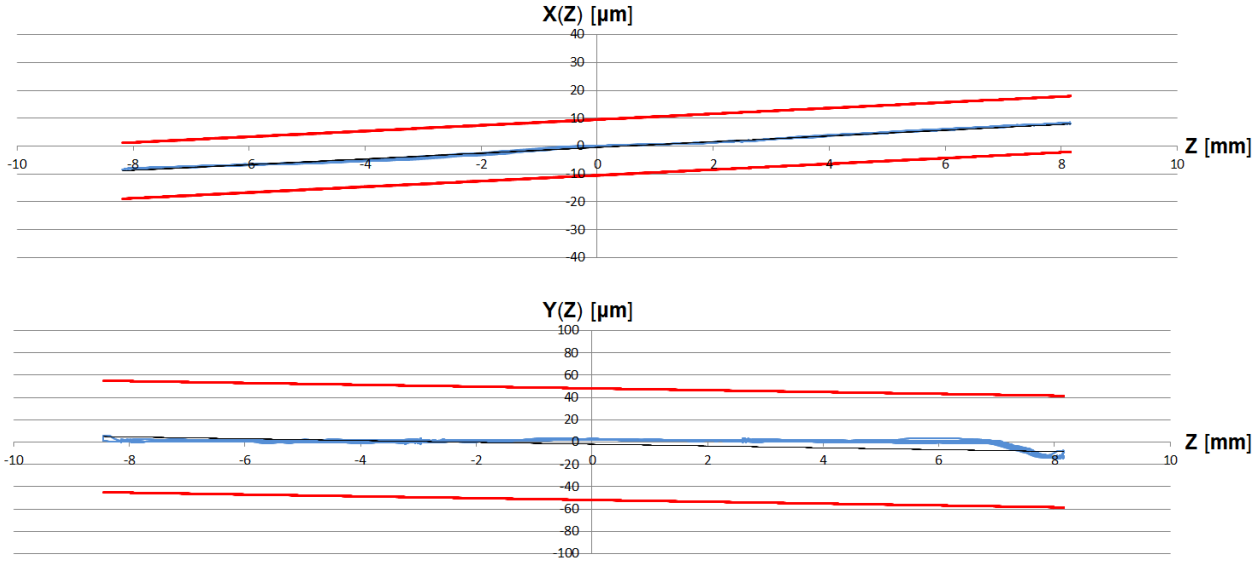

Figure 13. Slit carrier position in function of the Z-translation in mm

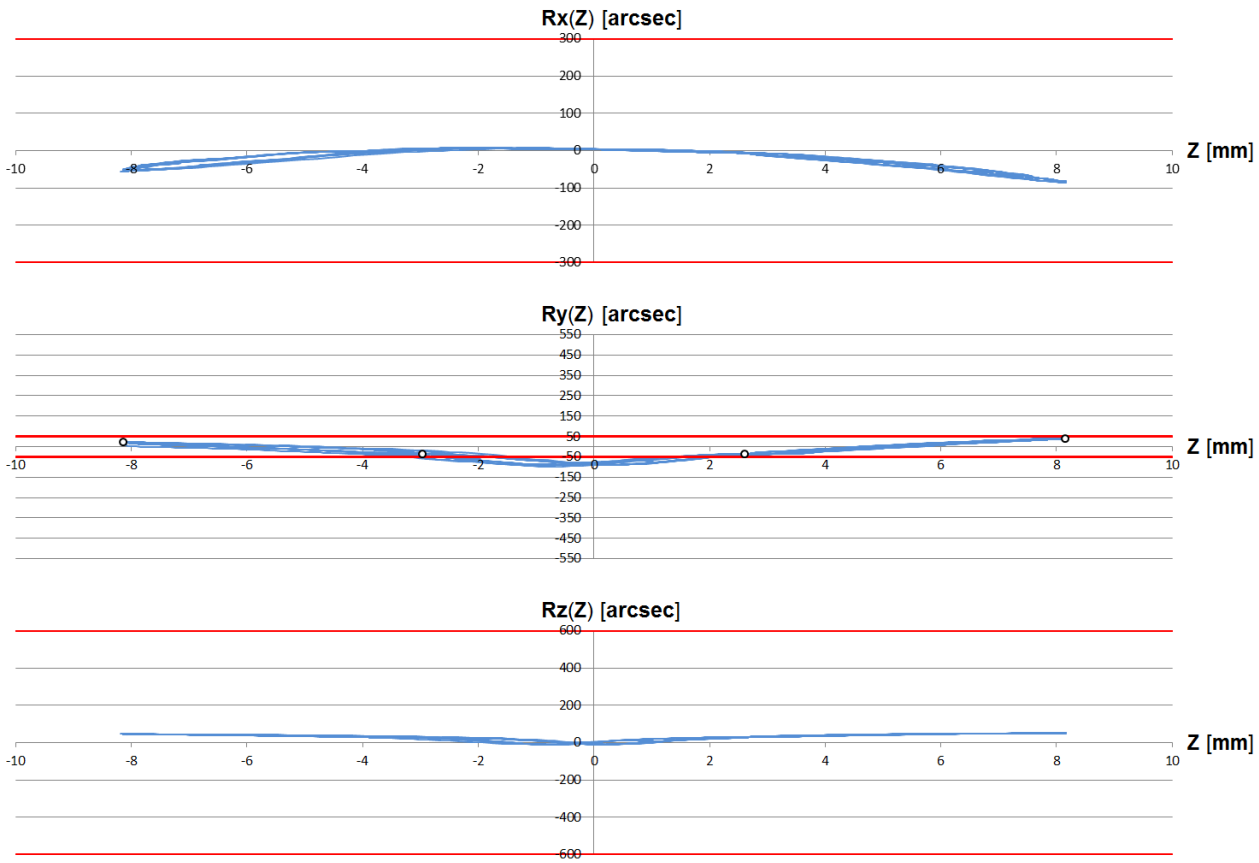

Figure 14. Slit carrier rotation in function of the Z-translation in mm

One potential enhancement of the flexible guiding system would be to connect both flexible blade ends together as they act as free pivot points (at +X and –X sides). However, this would make the design much more complex, in particular considering that these two additional mechanical structures would need to freely move along Z as well as to cope with the important launch environment and therefore be supported too. In any case, the requirements for the rotation around Y have been relaxed during the project. The design of the flexible guiding system with a connection rod is therefore considered fully suitable for the application and in compliance to the stringent positioning and repeatability requirements.

Table 7 summarizes the test results performed on flexible guiding system equipped with the compliant rod connection (breadboard model 2).

Table 7: Max positioning inaccuracy & worst case repeatability test results from Z-displacement

Direction	Position accuracy		Repeatability	
	Measured	Required	Measured	Required
X translation	±1.0 µm	±10 µm	±0.14 µm	±5 µm
Y translation	±8.5 µm	±50 µm	±2.36 µm	±3 µm
Rotation around X	±0.69 arcmin	±5 arcmin	±2.08 arcsec	±30 arcsec
Rotation around Y	±67 arcsec	±50 arcsec	±1.21 arcsec	±25 arcsec
Rotation around Z	±0.53 arcmin	±10 arcmin	±0.33 arcsec	±5 arcmin

Conclusions

The validation test results have demonstrated the full adequacy of the flexible blade guiding system implemented in SPICE's Slit Change Mechanism in a stand-alone configuration. Further breadboard test results, studying the influence of the compliant connection to the SCM linear actuator on an enhanced flexible guiding system design have shown significant enhancements in the positioning accuracy and repeatability of the selected flexible guiding system. Preliminary evaluation of the linear actuator design, including a detailed tolerance analyses, has shown the suitability of this satellite roller screw based mechanism for the actuation of the tested flexible guiding system and compliant connection.

The presented development and preliminary testing of the high-precision long-stroke Slit Change Mechanism for the SPICE Instrument are considered fully successful such that future tests considering the full Slit Change Mechanism can be performed, with the gained confidence, directly on a Qualification Model.

The selected linear Slit Change Mechanism design concept, consisting of a flexible guiding system driven by a hermetically sealed linear drive mechanism, is considered validated for the specific application of the SPICE instrument, with great potential for other special applications where contamination and high precision positioning are dominant design drivers.